J|A|C|S COMMUNICATIONS

Published on Web 10/15/2010

Solution Synthesis of Large-Scale, High-Sensitivity ZnO/Si Hierarchical Nanoheterostructure Photodetectors

Ke Sun,[†] Yi Jing,[†] Namseok Park,[†] Chun Li,[‡] Yoshio Bando,[‡] and Deli Wang*,[†]

Department of Electrical and Computer Engineering, University of California—San Diego, La Jolla, California 92093, United States, and International Center for Materials Nanoarchitectonics (MANA), National Institute for Material Science, Namiki 1-1, Tsukuba, Ibaraki 305-0044, Japan

Received May 5, 2010; E-mail: dwang@ece.ucsd.edu

Abstract: This Communication reports a low-cost solution fabrication of wafer-scale ZnO/Si branched nanowire heterostructures and their high photodetection sensitivity, with an ON/OFF ratio larger than 250 and a peak photoresponsivity of 12.8 mA/W at 900 nm. This reported unique 3D branched nanowire structure offers a generic approach for the integration of new functional materials for photodetection and photovoltaic applications.

Branched nanowires (NWs) are 3D nanoscale tree-like structures that consist of a NW core ("trunk") and NW "branches".[1] The formation of branched NWs offers direct homo- or heteroepitaxal[2] integration of materials with very different properties at the nanometer scale, which often lead to function integration or novel materials/applications. Moreover, 3D branched NW heterostructures offer greatly enhanced surface area and function and thus promise very attractive potential applications in optoelectronics, photocatalysis, photovoltaics, and sensing.[3] ZnO and Si are the most investigated NW materials.[4] ZnO is a direct band gap semiconductor with a wide band gap (E_g = 3.4 eV). It has a large exciton binding energy of 60 meV and is piezoelectric,[5] and thus it has been broadly studied for use in light-emitting diodes[6] and lasers,[7] photodetectors,[8] electrical generators,[9] photovoltaics,[10] transparent electrodes,[11] chemical and biological sensors,[12] etc. On the other hand, Si NWs have an indirect band gap of 1.12 eV and are piezoresistive; they have been intensively researched for applications as transistors,[13] logic circuits,[14] photodetectors,[15] photovoltaics,[16] chemical and biological sensors,[17] thermoelectric devices,[18] etc. Herein we report a low-cost, wafer-scale synthesis of ZnO/Si branched NW heterostructures and their application as high-sensitivity photodetectors. The direct integration of ZnO and Si and the growth of 3D branched NW heterostructures enable new functional materials to be synthesized for applications in optoelectronics, catalysis, and photovoltaics.

The Si NW core and ZnO NW branches were synthesized using simple and cost-effective aqueous solution methods. Both methods are applicable for large-scale synthesis. The wafer-scale Si NW arrays were obtained using a previously reported metal-assisted chemical etching process.[19] Figure 1a shows a scanning electron microscopy (SEM) image of NW arrays that were etched for 5 min on a 2-in. p-type Si wafer. SiNWs were about 680 nm in length, showing single-crystalline structure (Supporting Information). An optical image (Figure 1b) shows a very dark brownish color in the NW region, in significant contrast to the surrounding area that was covered from etching electrolyte, indicating that the light absorption was due to the waveguide effect.[16b] Light absorption was then

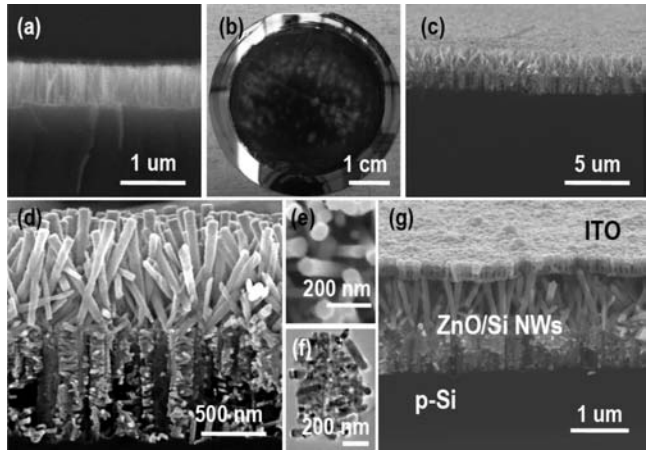

Figure 1. (a) Cross-sectional SEM image and (b) optical image of NW arrays on a 2 in. p-type Si wafer (etched for 5 min). (c) 45° view SEM micrographs of the ZnO/Si branched nanowire heterostructures at low magnification. (d) 89° view and (e) top view SEM micrographs of the ZnO/Si branched nanowire heterostructures at high magnification. (f) LR-TEM image on a single Si/ZnO branched NW. (g) 45° view SEM image of a photodetector device with top ITO contact.

further improved by integration of ZnO NWs on Si NW surfaces, revealed by reflectance evaluations. This enhancement is due to smoothing of the refraction index on going from the environment to the Si substrate. Hydrothermal growth of ZnO NWs is attractive due to its low reaction temperature and large-scale synthesis capability. Compared to gas-phase approaches, this method does not require expensive equipment, metal—organic source materials, or high temperatures. Hydrothermal growth of ZnO NWs on the seeded Si NW arrays was conducted according to the technique reported elsewhere.[10a] To ensure a uniform coating over the Si NW surface, low-pressure sputtering was used for seeding. The as-grown ZnO NW/Si NW heterostructures are shown in Figure 1c—e. Hexagonal ZnO NWs with diameter around 30 nm and very high density grow nearly perpendicular to the surface of the Si NW core and form highly ordered 3D branched NW heterostructures, as can be seen in a low-resolution transmission electron microscopy (LR-TEM) image (Figure 1f). It also appeared that the ZnO NWs grown on Si NW tips have larger diameter, presumably because there is less spatial hindrance and higher reactant concentration from diffusion. Devices were then fabricated by embedding the hetero-structure into an insulating polymer, followed by reactive ion etching (RIE) and top transparent contact deposition using indium tin oxide (ITO) and a Ti/Au probing pad (Figure 1g). Nanowire synthesis and fabrication procedures can be found in the Supporting Information.

[†] University of California—San Diego.
[‡] National Institute for Material Science, Japan.

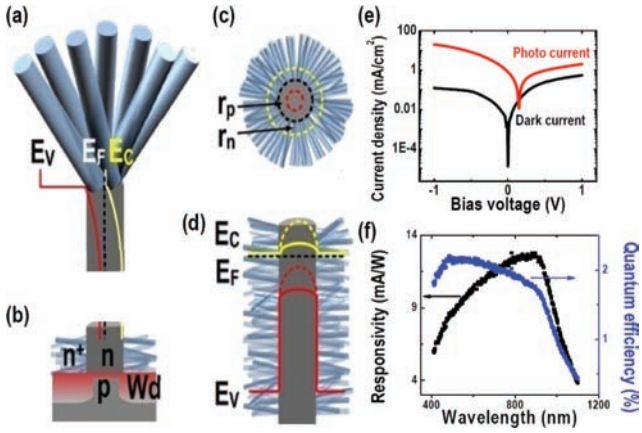

Figure 2. (a−d) Schematics of the ZnO/Si branched NW heterostructures: (a) top (NW tip) junction and energy band diagram; (b) bottom junctions and depletion layer in the silicon substrate; (c,d) cross-sectional view of the sidewall junctions and energy band diagram. (e) Current−voltage (I−V) characteristics measured in the dark and under xenon lamp illumination. (f) Spectral photoresponsivity and external quantum efficiency of ZnO/Si NW heterostructure photodetector from 400 to 1100 nm.

The current−voltage (I−V) characteristics of the Au/Ti/ITO/n-ZnO/p-Si/In device were tested in the dark and under illumination. Figure 2a−d illustrates the schematics of junctions along a single ZnO/Si NW heterostructure formed at different positions of the Si NW substrate, which are superimposed with the energy band diagrams. The carrier concentration was about 10^{18} cm^{-3} in ZnO NWs[10a] and about 10^{15} cm^{-3} in Si NWs. $\Delta E_C = 0$ eV and $\Delta E_V = 2.78$ eV were derived from the electron affinity and band gaps of ZnO and Si and confirmed by using a 1D Poisson solver[20] (Figure 2a,d). ZnO NWs had a carrier concentration 3 orders of magnitude higher than that of Si NWs. Therefore, the depletion width (r_p) was much larger in the Si NW core than in the ZnO branches (r_n) (Figure 2c), and the Si NWs were fully depleted and partially inverted to n-type (Figure 2d). p/n junctions were also formed between the ZnO NWs grown on Si substrate between the Si NWs, with larger depletion width (W_d) under the area between the Si NWs and smaller depletion width under the Si NWs, as shown in Figure 2b. Figure 2e shows the dark and photocurrent (under xenon lamp illumination) measurements at room temperature. Both dark and photocurrent voltage characteristics were rectifying, and the best ON/OFF ratio achieved at −1 V was about 250. Because of the clean interface between ZnO and Si NWs, the rectifying behavior was assigned to the ZnO/Si heterojunction and the Si substrate (Figure 2a−d). High-resolution TEM studies showed an oxide-free interface between ZnO and Si NWs (Figure S1, Supporting Information). A photovoltaic effect was observed, and the best solar cell device performance showed a power conversion efficiency under 1.5 a.m. solar simulator lumination of $\eta = 0.154\%$, with $J_{SC} = 4.1$ mA/cm^2, $V_{OC} = 0.15$ V, and FF = 0.25.

The spectral photoresponse of the ZnO/Si NW heterostructure device (400−1100 nm) was measured under a reserve bias of −1 V using a calibrated Si p-i-n photodiode (model 818-UV from Newport with OD3 attenuator) and monochromator (see Supporting Information for setup details). The photoresponsivity was calculated by calibrating the measured photocurrent density to that of the Si photodetector. Responsivity was calculated on the basis of eq 1,

$$R_\lambda = \frac{J_{ph}}{P_{inc}} = R_{\lambda det}\frac{J_{ph}}{J_{det}} \quad (1)$$

where R_λ and $R_{\lambda det}$ are the photoresponsivity of the ZnO/Si heterostructure device and calibration Si photodetector, respectively, J_{ph} and J_{det} are the measured current density from our device and the calibrated Si photodetector, and P_{inc} is the incident optical power. The external quantum efficiency (EQE) can be calculated by

$$\eta = R_\lambda \frac{q}{h\nu} = \frac{R_\lambda}{\lambda} \times 1240 \quad (2)$$

where η is the EQE, q, h, and υ are the electron charge, Planck's constant, and frequency of the incident photon, respectively, and λ is the wavelength. Figure 2f shows the photoresponsivity and EQE of the heterostructure device. The distinctive peak is the band edge absorption in the Si NW/substrate layer.[21] The maximum responsivity measured for this ZnO/Si heterostructure was as high as 12.8 mA/W at around 900 nm, and the maximum quantum efficiency was 2.20%.

In summary, ZnO/Si branched NW heterojunction photodiodes are fabricated using a cost-effective solution-phase process. This unique chemical integration of NW branches to vertical NW arrays promises enhanced light-trapping due to the aperiodically arranged nanowire array and high refractive index material filling, as well as advantages in broadband photon detection. Although ongoing research is addressing some of the challenging issues (such as uniform top contact and defects concentration) in order to further improve device performance, this unique branched NW heterostructure shows a peak responsivity of 12.8 mA/W at around 900 nm. These results indicate that the branched heterostructures, along with the wafer scale and low-cost solution processing, offer new functional materials for photodetection and photovoltaic cells.

Acknowledgment. D.W. acknowledges the U.S. DOE (DE-FG36-08G018016), NSF (ARRA ECCS0901113), the WCU program at Sunchon National University of South Korea, Abgent Inc., and AEM Inc. for financial support. The authors thank Dr. C. Soci of Nanyang Technology University of Singapore and W. Wei for useful discussions on the photoresponse measurement. K.S. thanks Dr. Y. Taur of UCSD for useful discussions.

Supporting Information Available: Nanowire synthesis and device fabrication procedures, TEM studies on the ZnO/Si interfaces, single SiNW device I−V measurement, electrical contact properties, and photoresponse measurements. This material is available free of charge via the Internet at http://pubs.acs.org.

References

(1) (a) Dick, K. A.; Deppert, K.; Larsson, M. W.; Martensson, T.; Seifert, W.; Wallenberg, L. R.; Samuelson, L. *Nat. Mater.* **2004**, *3*, 380–384. (b) Wang, D.; Lieber, C. M. *Nat. Mater.* **2003**, *2*, 355–356. (c) Wang, D.; Qian, F.; Yang, C.; Zhong, Z.; Lieber, C. M. *Nano Lett.* **2004**, *4*, 871–874.
(2) (a) Jiang, Y.; Zhang, W. J.; Jie, J. S.; Meng, X. M.; Zapien, J. A.; Lee, S. T. *Adv. Mater.* **2006**, *18*, 1527–1532. (b) Jung, Y.; Ko, D.-K.; Agarwal, R. *Nano Lett.* **2006**, *7*, 264–268.
(3) (a) Bae, S. Y.; Seo, H. W.; Choi, H. C.; Park, J.; Park, *J. Phys. Chem. B* **2004**, *108*, 12318–12326. (b) Lao, J. Y.; Wen, J. G.; Ren, Z. F. *Nano Lett.* **2002**, *2*, 1287–1291. (c) Li, Y.; Gong, J.; Deng, Y. *Sensors Actuators A* **2010**, *158*, 176–182. (d) Mudusu, D.; Nandanapalli Koteeswara, R.; Alexander, P.; Fernando, P. *ChemPhysChem* **2010**, *11*, 809–814. (e) Wang, N.; Sun, C.; Zhao, Y.; Zhou, S.; Chen, P.; Jiang, L. *J. Mater. Chem.* **2008**, *18*, 3909–3911. (f) Xu, F.; Dai, M.; Lu, Y.; Sun, L. *J. Phys. Chem. C* **2010**, *114*, 2776–2782. (g) Bierman, M. J.; Jin, S. *Energy Environ. Sci.* **2009**, *2*, 1050–1059.
(4) Hochbaum, A. I.; Yang, P. *Chem. Rev.* **2009**, *110*, 527–546.
(5) Wang, Z. L.; Song, J. *Science* **2006**, *312*, 242–246.
(6) Bao, J.; Zimmler, M. A.; Capasso, F.; Wang, X.; Ren, Z. F. *Nano Lett.* **2006**, *6*, 1719–1722.
(7) Mariano, A. Z.; Jiming, B.; Federico, C.; Sven, M.; Carsten, R. *Appl. Phys. Lett.* **2008**, *93*, 051101.
(8) Soci, C.; Zhang, A.; Xiang, B.; Dayeh, S. A.; Aplin, D. P. R.; Park, J.; Bao, X. Y.; Lo, Y. H.; Wang, D. *Nano Lett.* **2007**, *7*, 1003–1009.
(9) Xu, S.; Qin, Y.; Xu, C.; Wei, Y.; Yang, R.; Wang, Z. L. *Nat. Nanotechnol.* **2010**, *5*, 366–373.
(10) (a) Law, M.; Greene, L. E.; Johnson, J. C.; Saykally, R.; Yang, P. *Nat. Mater.* **2005**, *4*, 455–459. (b) Yang, X.; Wolcott, A.; Wang, G.; Sobo, A.;

Fitzmorris, R. C.; Qian, F.; Zhang, J. Z.; Li, Y. *Nano Lett.* **2009**, *9*, 2331–2336.
(11) Lee, S.-H.; Han, S.-H.; Jung, H. S.; Shin, H.; Lee, J.; Noh, J.-H.; Lee, S.; Cho, I.-S.; Lee, J.-K.; Kim, J.; Shin, H. *J. Phys. Chem. C* **2010**, *114*, 7185–7189.
(12) Yang, K.; She, G.-W.; Wang, H.; Ou, X.-M.; Zhang, X.-H.; Lee, C.-S.; Lee, S.-T. *J. Phys. Chem. C* **2009**, *113*, 20169–20172.
(13) Cui, Y.; Zhong, Z.; Wang, D.; Wang, W. U.; Lieber, C. M. *Nano Lett.* **2003**, *3*, 149–152.
(14) Zhong, Z.; Wang, D.; Cui, Y.; Bockrath, M. W.; Lieber, C. M. *Science* **2003**, *302*, 1377–1379.
(15) Yang, C.; Barrelet, C. J.; Capasso, F.; Lieber, C. M. *Nano Lett.* **2006**, *6*, 2929–2934.
(16) (a) Kelzenberg, M. D.; Boettcher, S. W.; Petykiewicz, J. A.; Turner-Evans, D. B.; Putnam, M. C.; Warren, E. L.; Spurgeon, J. M.; Briggs, R. M.; Lewis, N. S.; Atwater, H. A. *Nat. Mater.* **2010**, *9*, 239–244. (b) Zhu, J.; Yu, Z.; Burkhard, G. F.; Hsu, C.-M.; Connor, S. T.; Xu, Y.; Wang, Q.; McGehee, M.; Fan, S.; Cui, Y. *Nano Lett.* **2008**, *9*, 279–282. (c) Hu, L.; Chen, G. *Nano Lett.* **2007**, *7*, 3249–3252. (d) Tian, B.; Zheng, X.; Kempa, T. J.; Fang, Y.; Yu, N.; Yu, G.; Huang, J.; Lieber, C. M. *Nature* **2007**, *449*, 885–889.
(17) Zheng, G.; Patolsky, F.; Cui, Y.; Wang, W. U.; Lieber, C. M. *Nat. Biotechnol.* **2005**, *23*, 1294–1301.
(18) Hochbaum, A. I.; Chen, R.; Delgado, R. D.; Liang, W.; Garnett, E. C.; Najarian, M.; Majumdar, A.; Yang, P. *Nature* **2008**, *451*, 163–167.
(19) Peng, K. Q.; Yan, Y. J.; Gao, S. P.; Zhu, *Adv. Mater.* **2002**, *14*, 1164–1167.
(20) Snider, G., 1D Poisson solver, http://www.nd.edu/∼gsnider/.
(21) Chen, L. C.; Pan, C. N. *Eur. Phys. J. Appl. Phys.* **2008**, *44*, 43–46.

JA1038424